

**\*\*FULL TITLE\*\***  
*ASP Conference Series, Vol. \*\*VOLUME\*\*, \*\*YEAR OF PUBLICATION\*\**  
**\*\*NAMES OF EDITORS\*\***

## Characteristics of the Galactic magneto-ionized ISM from Faraday rotation

Marijke Haverkorn

*Jansky fellow, National Radio Astronomy Observatory*

*Astronomy Department University of California at Berkeley, 601  
 Campbell Hall, Berkeley CA 94720, USA*

**Abstract.** Faraday rotation measurements of polarized extragalactic sources probe the Galactic magnetized, ionized interstellar medium. Rotation measures of these sources behind the inner Galactic plane are used to explore characteristics of the structure in the spiral arms and in interarm regions. Structure in the spiral arms has a characteristic outer scale of a few parsecs only, whereas interarm regions typically show structure up to scales of hundreds of parsecs. The data indicate that in the spiral arms, the random component of the magnetic field dominates over the regular field, but in the interarm regions the random and regular field components may be comparable, and a few times weaker than the random magnetic field in the spiral arms.

### 1. Introduction

The discussion whether tiny scale structure in atomic, molecular or ionized form is part of a power law power spectrum or is made up of overdense discrete structures is ongoing (see e.g. Heiles, Mason, Deshpande, this volume). Therefore, in addition to the study of the tiny structures themselves, studies to determine the power spectra of the neutral and ionized medium are relevant to have a framework in which the existence of tiny scale structure can be tested.

The velocity and density power spectra of neutral gas are extensively probed as part of molecular cloud evolution and star formation studies (Elmegreen & Scalo 2004). For the warm ionized component of the interstellar medium (ISM), electron density studies mostly show Kolmogorov spectra (Armstrong et al. 1995). The ionized gas dynamics and structure are expected to be heavily influenced by magnetic fields threading the medium, the characteristics of which are still very uncertain.

In this paper, we discuss fluctuations in the warm magneto-ionized medium probed by way of Faraday rotation, to estimate typical scales of structure and magnetic field strengths in spiral arms and in interarm regions.

### 2. Data analysis of polarized extragalactic point sources

Polarized radiation from extragalactic point sources is altered by Faraday rotation when propagating through the Milky Way plane, which makes these point

sources a good probe of the structure in the Galaxy's magnetic field and electron density.<sup>1</sup>

However, as these sources are irregularly spaced on the sky, performing a Fourier transform to obtain the typical scales of structure introduces artifacts. Instead, the second order structure function (SF) of rotation measure RM can be used, which is defined as  $D_{\text{RM}}(dr) = \langle (\text{RM}(r) - \text{RM}(r + dr))^2 \rangle_r$ , where  $dr$  is the separation of two sources on the sky, and  $\langle \rangle_r$  is an average over every position  $r$  which contains a source with a neighboring source in a bin around  $dr$  away. For a power law power spectrum in RM, the SF will be a power law with a certain smallest dissipation scale  $l_d$  which is much smaller than the scales probed in this paper, and an outer scale  $l_0$  which is the maximum scale found in the turbulence, believed to be the dominant scale of energy input.

The data we use are from the Southern Galactic Plane Survey (SGPS, McClure-Griffiths et al. 2005, Haverkorn et al. 2006a), a neutral hydrogen and full-polarization 1.4 GHz continuum survey of the Galactic plane, which spans an area of  $253^\circ < l < 357^\circ$  and  $|b| < 1.5^\circ$  and contains 148 polarized sources with an unambiguous RM measurement (Brown et al. 2006). The data are obtained with the Australia Telescope Compact Array (ATCA) and the Parkes 64m single-dish telescope, and are publicly available (ATCA data only for polarized continuum data)<sup>2</sup>.

Lines of sight through discrete structures like H II regions and supernova remnants are biased due to the large electron density and possibly magnetic field, which increases  $|\text{RM}|$  in this direction (Mitra et al. 2003). Therefore, we have used the total intensity 1.4 GHz radio data from the ATCA combined with Parkes single-dish data to determine which extragalactic sources have a sight line passing through a supernova remnant or H II region. The data from these sources (about 15% of the total sample) were then discarded.

SFs are sensitive to large-scale gradients in electron density across the field of view. In addition, the geometrical component of the change in magnetic field can to first order be approximated with a linear contribution. A plane in RM is subtracted from the area in which a SF is computed to correct for these effects.

Because the SGPS data probe the inner Galaxy, which includes a number of spiral arms, they are well-suited to study differences in the structure in the ISM in spiral arms and in interarm regions. The SGPS sources are used to construct SFs for different lines of sight preferentially through spiral arms or mostly through interarm regions, estimated from the spiral arm positions in Cordes & Lazio (2002). Figure 1 shows the SFs in lines of sight primarily going through interarm regions (upper panels) and in lines of sight dominated by spiral arms (lower panels).

---

<sup>1</sup>Faraday rotation describes the rotation of the angle of linear polarization  $\phi$  due to birefringence for left and right handed circular polarization in a magnetized, ionized medium. Faraday rotation is wavelength dependent:  $\phi \propto \text{RM} \lambda^2$ , where rotation measure RM is  $\text{RM} = 0.81 \int n_e [\text{cm}^{-3}] B_{\parallel} [\mu\text{G}] dl [\text{pc}]$ , with  $n_e$  thermal electron density,  $B_{\parallel}$  magnetic field strength parallel to the line of sight and  $dl$  path length.

<sup>2</sup><http://www.atnf.csiro.au/research/cont/sgps/queryForm.html>

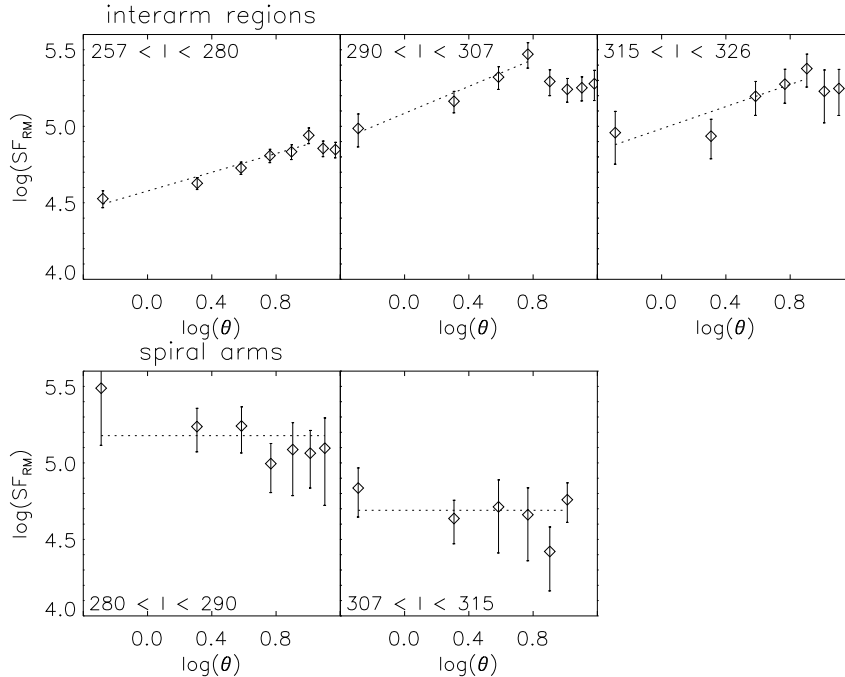


Figure 1. Structure functions of RM for Galactic interarm regions (top) and spiral arms (bottom). The dotted lines are linear fits to the rising parts of the SFs (top) and horizontal lines (bottom).

### 3. Typical scales of structure

#### 3.1. The turnover scale of structure functions

The difference between the structure in RM in spiral arms and the structure in interarm regions is obvious: the spiral arm SFs are flat, while in interarm regions the SFs rise to a certain turnover in the SF. The location of the turnover is interpreted as the largest angular scale of structure in the interarm regions. With the argument that the largest angular scales in RM are probably coming from nearby, this outer scale corresponds to spatial scales of about 100-200 pc. For the spiral arms we can only estimate an upper limit for the outer scale of structure, i.e. the smallest scale we probe. In this way, we estimate the outer scale of structure in the spiral arms to be smaller than about 10 pc (Haverkorn et al. 2006b).

#### 3.2. Depolarization of point sources

An independent estimate of the outer scales of the structure can be made from depolarization of extragalactic point sources. This depolarization is caused by variability in polarization angle on angular scales smaller than the size of the (unresolved) source. The variance in polarization angle within a telescope beam will decrease the polarization degree of the source.

Variations in polarization angle causing partial depolarization are expected to arise within any polarized extragalactic source itself. Indeed, no source in our sample exhibits the intrinsic maximum degree of polarization of around 70%, but instead observed polarization degrees are typically under 10%. However, a

region	range in $l$ [ $^{\circ}$ ]	$r_{out}$ [pc]	$p$ [%]	$\sigma$ [rad m $^{-2}$ ]	$r_{out}^d$ [pc]	$B_0$ [ $\mu$ G]	$C_B^2$	$B_{ran}$ [ $\mu$ G]
Inter1	255 - 281	100	5.5	200	1	2.8	10	2.1
Carina	281 - 292	< 17	1.5	250	7	3.5	18	2.8
Inter2	292 - 308	170	3.7	250	3	3.8	3	1.2
Crux	308 - 317	< 40	3.3	160	6	3.2	100	6.7
Inter3	317 - 327	220	2.5	225	5	3.7	100	6.7

Table 1. ISM parameters for three interarm regions and the Carina and Crux spiral arms. The parameter  $r_{out}$  is the outer scale determined from the turnover of the structure functions;  $p$  is observed polarization degree, and  $\sigma$  is the standard deviation in RM. The outer scale as determined from depolarization is given by  $r_{out}^d$ ,  $B_0$  is the parallel component of the regular magnetic field,  $C_B^2$  is the amplitude of the magnetic field spectrum given in  $10^{-13} \text{ m}^{-2/3} \mu\text{G}^2$ , and  $B_{ran}$  the resulting random magnetic field strength.

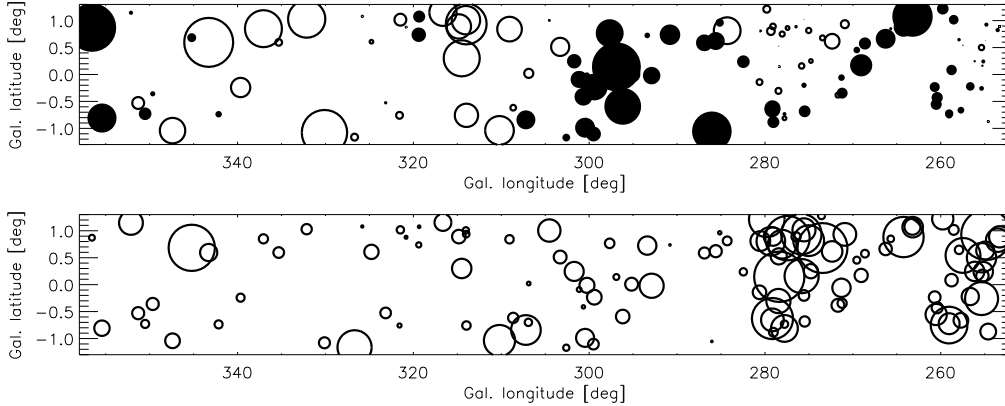


Figure 2. Top: SGPS field of view, where the circles are RMs of extragalactic sources. RM minimum and maximum is  $\pm 1000 \text{ rad m}^{-2}$ . Bottom: same field and same sources, but the circles denote degree of polarization. Minimum degree of polarization is 0.4%, the maximum 13.7%.

Galactic component to this depolarization has been detected as well. Figure 2 shows RMs in the upper panel and polarization degree  $p$  in the bottom panel, and a clear anticorrelation between  $|\text{RM}|$  and  $p$  is visible especially at the lower longitudes. This trend is also evident in Figure 3, which shows the degree of polarization of every source as a function of its RM. As the scale of the structure in RM and  $p$  is several degrees, this cannot be intrinsic to the sources but instead must be caused by the Galactic ISM.

The Galactic component of this depolarization can be estimated assuming a power-law power spectrum of RM fluctuations, in the approximation that the outer scale of structure  $r_{out}$  is much larger than the source size  $r_{src}$  which is the case here. Adapted from Tribble (1991), the depolarization by a power spectrum of RM fluctuations is given by the degree of polarization  $p$  as:

$$\left\langle \left| \frac{p(\lambda)}{p_0} \right|^2 \right\rangle \approx 1 - 4\sigma^2 \lambda^4 2^{m/2} \left( \frac{r_{src}}{r_{out}} \right)^m \Gamma\left(1 + \frac{m}{2}\right) \quad (1)$$

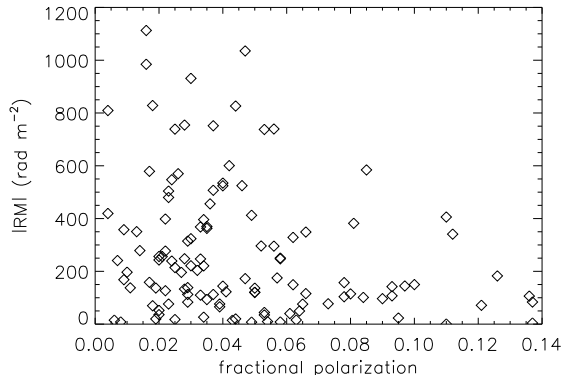


Figure 3. Polarization degree  $p$  against  $|RM|$  for each source.

where  $p_0$  is the intrinsic polarization degree of the extragalactic source radiation when it exits the source and  $\sigma$ ,  $m$  and  $r_{out}$  are defined via the structure function

$$D_{RM}(r) = \begin{cases} 2\sigma^2(r/r_{out})^m & \text{for } r < r_{out} \\ 2\sigma^2 & \text{for } r > r_{out} \end{cases}$$

The average degree of polarization in the studied regions is given in Table 1. The spiral arms seem to be more depolarized than the interarm regions, with some possible confusion closest to the Galactic center due to superposition of arms and interarm regions along the line of sight.

The amount of intrinsic depolarization resulting in polarization degree  $p_0$  can be estimated from the extragalactic sources observed in and around the LMC (Gaensler et al. 2005) to be 10.4%, which we assume is the average polarization degree of point sources for which all depolarization is intrinsic. With these assumptions, the depolarization beyond 10.4% is due to the variations in Galactic RM across the face of the source, which is on average 6 arcsec (Gaensler et al. 2005). This percentage is higher than the actual average degree of polarization due to a selection of strong, highly-polarized sources over weak, weakly polarized ones. However, as we are interested in the relative depolarization only, this selection effect does not influence our conclusions.

In the spiral arms it is straightforward to use Eq. (1) to obtain the outer scale  $r_{out}^d$  needed to obtain the observed depolarization. We assume Kolmogorov turbulence ( $m = 5/3$ , however, see Section 5.), and determine the value of the RM standard deviation  $\sigma$  from the SF saturation level. The distance is chosen to be the average distance to the region probed, which has a large error due to the large spatial extent of the gas.

For the interarm regions we observe a shallow spectrum. Assuming that this spectrum turns over to a steeper Kolmogorov spectrum towards small scales (see Section 4.), the Kolmogorov slope on small scales will dominate the depolarization of the point sources. Then, using linear fits to the rising parts of the slopes, we can calculate at which  $r_{out}$  and  $\sigma_{RM}$  the depolarization given by Eq. (1) equals the observed depolarization in Table 1. This  $r_{out}$  is the outer scale of the Kolmogorov turbulence, i.e. the scale at which the Kolmogorov slope turns over into a shallower slope. This scale is given in Table 1 as the  $r_{out}^d$  in the interarm

regions, and is consistent with the outer scale of Kolmogorov turbulence found in the spiral arms of a few parsecs.

#### 4. Amplitude of magnetic field fluctuations

While the turnover in the SF of RM corresponds to the outer scale of structure, the *amplitude* of the SF gives information about the magnitude of the magnetic field fluctuations in the medium.

Minter & Spangler (1996, MS96) developed a formalism with which to describe the SF of RM assuming power spectra in magnetic field and in electron density fluctuations which are zero-mean, isotropic and Gaussian. Assuming Kolmogorov turbulence, MS96 find that the RM structure function can be described as:

$$D_{RM} = [251.226 \left[ \left( \frac{n_0}{0.1 \text{ cm}^{-3}} \right)^2 \left( \frac{C_B^2}{10^{-13} \text{ m}^{-2/3} \mu\text{G}^2} \right) + \left( \frac{B_0}{\mu\text{G}} \right)^2 \left( \frac{C_n^2}{10^{-3} \text{ m}^{-20/3}} \right) \right] + 23.043 \left( \frac{C_n^2}{10^{-3} \text{ m}^{-20/3}} \right) \left( \frac{C_B^2}{10^{-13} \text{ m}^{-2/3} \mu\text{G}^2} \right) \left( \frac{l_0}{\text{pc}} \right)^{2/3} ]^* \left( \frac{L}{\text{kpc}} \right)^{8/3} \left( \frac{\delta\theta}{\text{deg}} \right)^{5/3}$$

where  $n_0$  is the mean electron density,  $B_0$  is the mean magnetic field strength along the line of sight,  $l_0$  the outer scale of structure,  $L$  the length of the line of sight and the magnetic field and density fluctuations are described by power laws with the same outer scale and spectral index such that

$$\langle \delta B_i(\mathbf{r}_0) \delta B_i(\mathbf{r}_0 + \mathbf{r}) \rangle = \int d^3q \frac{C_B^2 e^{-i\mathbf{q}\cdot\mathbf{r}}}{(q_0^2 + q^2)^{\alpha/2}}$$

and a similar expression for  $\langle \delta n(\mathbf{r}_0) \delta n(\mathbf{r}_0 + \mathbf{r}) \rangle$ . Assuming that on smaller scales the magnetic field power spectrum follows the observed Kolmogorov spectrum of electron density, the observed SFs will turn over to steeper slopes towards smaller scales. The constraint that the Kolmogorov SF on the small scales and the shallower SF on larger scales must have the same amplitude at turnover scale  $l_0$  yields

$$D_{RM}(\delta\theta) = \begin{cases} A\delta\theta^{5/3} & \text{for } \delta\theta \leq l_0/L \\ A\delta\theta^m(l_0/L) & \text{for } \delta\theta \geq l_0/L \end{cases}$$

where  $m$  is the spectral index of the shallower SF. Following this formalism, we can derive the amplitude of the magnetic field fluctuations in the spiral arms and interarm regions, which is shown as the dotted lines in Figure 1, while the input and output parameters for the computation are given in Table 1. The mean electron density was determined from the Cordes & Lazio (2002) electron density model,  $B_{\parallel}$  was calculated assuming a constant circular field with a strength  $B_{reg} = 4 \mu\text{G}$  (Beck et al. 1996), and the outer scale of Kolmogorov turbulence  $r_{out}$  is taken as 5 pc in both arms and interarms, consistent with the rough estimates in Table 1. The path length is chosen as the distance to the point for which 90% of the electron density along the line of sight is contained in the path length.

This procedure allows us to calculate the random magnetic field coefficient  $C_B^2$  and the corresponding random magnetic field strengths of about  $7 \mu\text{G}$  in the spiral arms and  $2 \mu\text{G}$  in the interarm regions, see Table 1. Caution needs to be taken that the uncertainties in the input parameters are large so that the magnetic field strength values are also fairly uncertain. However, the analysis indicates that the random magnetic field component is consistent with a constant in all interarm regions much lower than the value in the spiral arms.

Random magnetic field strength in the spiral arms exceeding that in the interarms has been observed in some external galaxies (e.g. NGC 4631, Beck & Hoernes 1996; IC342, Krause, Hummel & Beck 1989), although the situation is not clear in the Milky Way. It is expected for spiral galaxies with weak dynamos (Shukurov 1998).

## 5. Speculations on the nature of the structure

If the above assumption is correct and the computed SFs will turn over to a (steeper) Kolmogorov spectrum at smaller scales, several mechanisms can be responsible for creating the shallow slopes.

Superposition of two spiral arms with similar spatial outer scales at different distances will yield a shallow transition SF at scales just smaller than the saturation scale. However, lines of sight with more spiral arm superpositions (higher longitude) should give shallower spectra, contrary to what is observed. Furthermore, other observations in the outer Galactic plane (Sun & Han 2004) and at higher Galactic latitudes (Haverkorn et al. 2003) which find shallow slopes without possible spiral arm superpositions argue against this explanation.

Discrete structures with internal turbulence within a turbulent medium, such as H II regions, can also explain the observations. In this case, on small scales (i.e. scales smaller than the size of the region) turbulence in the H II regions would dominate the SF, whereas on larger scales these clouds would just add a constant 'noise' term, which makes the total slope shallower.

Shallow SF slopes can also be caused by a transition from 2D to 3D turbulence as suggested by MS96. They invoke physical sheets of gas in which turbulence cannot operate perpendicular to the sheets, which is a logical choice for the region of the sky that they probe, which has a large H II region near by. For data over a significant part of the plane, this interpretation is not likely.

A plausible option is multiple scales of energy input in the interarm regions: for supernova-driven turbulence, the outer scale is believed to be about 100 pc (as observed). However, if energy sources such as stellar winds or outflows, interstellar shocks or H II regions input a significant amount of energy into the interstellar turbulence on smaller scales (typically parsecs, Mac Low 2004), this may flatten the SF on scales of order 1 pc to scales of order 100 pc, as observed.

Alternatively, the power spectrum of magnetic field fluctuations may not follow the Kolmogorov scaling at all. If this is the case, the difference between spiral arms and interarm regions may be due to the absence and presence of a strong regular magnetic field in the arms and interarms, respectively, causing a different spectral index (e.g. Schekochihin et al. 2004), or due to a transition between subsonic and supersonic turbulence.

## 6. Summary and conclusions

Faraday rotation measurements of polarized extragalactic sources behind the inner Galactic plane in the fourth quadrant are used to study the characteristics of the magnetized, ionized interstellar medium in the plane, in particular in the spiral arms and in interarm regions. Structure functions show that the typical outer scale of structure in the spiral arms is a few parsecs, whereas in the interarm regions fluctuations up to hundreds of parsecs in size are observed. Partial depolarization of the extragalactic sources by the ISM is used to derive a turbulent outer scale of a few parsecs, assuming Kolmogorov-like turbulence. From the saturation amplitudes of the structure functions the strength of the random magnetic field component in the spiral arms and interarm regions is estimated. Assuming an equal regular magnetic field strength in both arms and interarms, it is found that the random field in the arms is about 3 times stronger than that in the interarm regions. In this case, the random magnetic field dominates in the spiral arms, whereas the regular and random components are similar in the interarm regions.

**Acknowledgments.** The ATCA is part of the Australia Telescope, which is funded by the Commonwealth of Australia for operation as a National Facility managed by CSIRO. The author would like to thank Bryan Gaensler, Jo-Anne Brown, Alexander Schekochihin, Stanislav Boldyrev, Steve Spangler, and Joel Weisberg for stimulating discussions. M.H. acknowledges support from the National Radio Astronomy Observatory (NRAO), which is operated by Associated Universities Inc., under cooperative agreement with the National Science Foundation.

## References

- Armstrong, J. W., Rickett, B. J., & Spangler, S. R. 1995, *ApJ*, 443, 209  
 Beck, R., Brandenburg, A., Moss, D., et al. 1996, *ARA&A*, 34, 155  
 Beck, R., & Hoernes, P. 1996, *Nat*, 379, 47  
 Brown, J. C., Haverkorn, M., Gaensler, B. M., Taylor, A. R., et al. 2006, *ApJL* submitted  
 Cordes, J. M., & Lazio, T. J. W. 2002, preprint (astro-ph/0207156)  
 Elmegreen, B. G., & Scalo, J. 2004, *ARA&A*, 42, 211  
 Gaensler, B.M., Haverkorn, M., Staveley-Smith, L., et al. 2005, *Science*, 307, 1610  
 Haverkorn, M., Gaensler, B. M., McClure-Griffiths, N. M., et al. 2006a, *ApJ*, in press  
 Haverkorn, M., Gaensler, B. M., Brown, J. C., Bizunok, N., et al. 2006b, *ApJL*, 637, 33  
 Haverkorn, M., Katgert, P., de Bruyn, A. G. 2003, *A&A*, 403, 1045  
 Krause, M., Hummel, E., & Beck, R. 1989, *A&A*, 217, 4  
 Mac Low, M.-M. 2004, *Ap&SS*, 289, 323  
 McClure-Griffiths, N. M., Dickey, J. M., Gaensler, B. M., et al. 2005, *ApJS*, 158, 178  
 Minter, A. H., & Spangler, S. R. 1996, *ApJ*, 458, 194  
 Mitra, D., Wiełebinski, R., Kramer, M., & Jessner, A. 2003, *A&A*, 398, 993  
 Schekochihin, A. A., Cowley, S. C., Taylor, S. F., et al. 2004, *ApJ*, 612, 276  
 Shukurov, A. 1998, *MNRAS*, 299, 21  
 Sun, X. H., & Han, J. L. 2004, in *The Magnetized Interstellar Medium*, ed. B. Uyaniker, W. Reich, R. Wiełebinski (Katlenburg-Lindau: Copernicus GmbH), 25  
 Tribble, P. C. 1991, *MNRAS*, 250, 726